

## Ti-Si-N films prepared by magnetron sputtering

PAN Li<sup>a, b</sup>, BAI Yizhen<sup>a</sup>, ZHANG Dong<sup>a</sup>, and WANG Jian<sup>a</sup><sup>a</sup> Key Laboratory of Materials Modification by Laser, Ion and Electron Beams, Ministry of Education, School of Physics and Optoelectronic Technology, Dalian University of Technology, Dalian 116024, China<sup>b</sup> PLA No. 5311 Factory, Nanjing 211100, China

Received 7 July 2011; received in revised form 20 October 2011; accepted 2 November 2011

© The Nonferrous Metals Society of China and Springer-Verlag Berlin Heidelberg 2012

### Abstract

A film growth mechanism, expressed in terms of depositing hard films onto the soft substrate, was proposed. Multicomponent thin films of Ti-Si-N were deposited onto Al substrate with a double-target magnetron sputtering system in an Ar-N<sub>2</sub> gas mixture. The Ti-Si-N films were investigated by characterization techniques such as X-ray diffraction (XRD), atomic force microscope (AFM), electron probe microanalyzer (EPMA), scratch test and nanoindentation. The as-deposited films have a good adhesion to Al substrate and appear with smooth and lustrous surface. The films show nanocomposite structure with nano TiN grains embedded in an amorphous SiN<sub>x</sub> matrix. The maximum hardness of the films was achieved as high as 27 GPa. The influences of the N<sub>2</sub> flow rate and substrate temperature on the growth rate and quality of the films were also discussed. For all samples, the Ar flow rate was maintained constant at 10 ml·min<sup>-1</sup>, while the flow rate of N<sub>2</sub> was varied to analyze the structural changes related to chemical composition and friction coefficient. The low temperature in the deposited Ti-Si-N films favors the formation of crystalline TiN, and it leads to a lower hardness at low N<sub>2</sub> flow rate. At the same time, the thin films deposited are all crystallized well and bonded firmly to Al substrate, with smooth and lustrous appearance and high hardness provided. The results indicate that magnetron sputtering is a promising method to deposit hard films onto soft substrate.

**Keywords:** Ti-Si-N films; nanocomposite; nanoindentation; hardness

## 1 Introduction

Aluminium alloys are potential materials used in space technology and many other fields due to their well-known properties. But the blare of the surface and the hardness are very poor; meanwhile the friction coefficient of Al is very high, especially under the high vacuum environment [1–2]. With the development of modern industry, it's necessary to make an advanced investigation on the quality and performance of Al surface. Aluminium alloys neither have a good surface adhesion to its films [3–4] nor form a compact film on its surface under the influence of high active surface. Therefore, it's a significant subject to find a proper surface technique and protected material in the improved material field of soft substrate [5]. So, when they are used in strong friction conditions, they are usually needed to be coated with protective hard films [1]. However, it is difficult to grow hard films on the Al substrate due to their poor adhesion. Therefore, it's a significant subject to find a proper surface technique and protective material in the surface modification field of soft metal substrates.

Ti-Si-N films have attracted people's interest for many

years due to their outstanding mechanical properties such as high hardness, low wear coefficient, and high chemical stability [6–9]. Currently, deposition of thin films by reactive magnetron sputtering is the most popular technique for synthesizing two-phase nanocomposite Ti-Si-N films because of its several intrinsic advantages over thermal CVD and PECVD [10–12]. But, up to now, studies about Ti-Si-N films focus on the protection of high-speed steel [13–15], stainless steel [10, 16–17], cemented carbides [18–19], silicon [11, 20] and other hard substrates [21]. There are rare reports of their preparation on the soft substrates. The results in this paper are not only useful for understanding of the structural and compositions of Ti-Si-N films, but more importantly also put forward a solution to the adhesion between hard films and soft substrates.

The main objective of this work was to prepare Ti-Si-N films onto the soft metal substrate. Ti-Si-N films were first deposited onto Al substrates by magnetron sputtering. Furthermore, we introduce into the Si substrate for the sake of measuring the thickness and other property of the films more conveniently. Then the microstructure, morphologies and compositions of the films were measured by XRD,

AFM and EPMA, respectively. At the same time, the mechanical properties including nanohardness, Young's modulus, and friction coefficient were also examined.

## 2 Experimental

Ti-Si-N films were deposited onto Si and Al substrates by a double-target magnetron sputtering system in a mixed atmosphere of nitrogen ( $N_2$ ) and argon (Ar) with different  $N_2$  flow rates. In this study, the schematic of the magnetron sputtering system used for the deposition was shown in Fig. 1. This equipment was designed to prepare new materials by co-sputtering double targets. The rotation of specimen holder guarantees a uniform growth of the films. Direct current (DC) and radio frequency (RF) power supply were used for Ti target and Si target, respectively. A substrate holder was located 110 mm away from the targets. In order to get rid of the surface contamination, the Al substrates were grinded mechanically before polished to specular surfaces. Afterwards, they were ultrasonically cleaned in acetone and absolute ethanol for 10 min in sequence. All the substrates were taken off the oxidated layer to ensure that each one has the identical surface characteristic and crystalline orientation. Finally, they were dried by nitrogen gas and then placed into the vacuum chamber immediately.

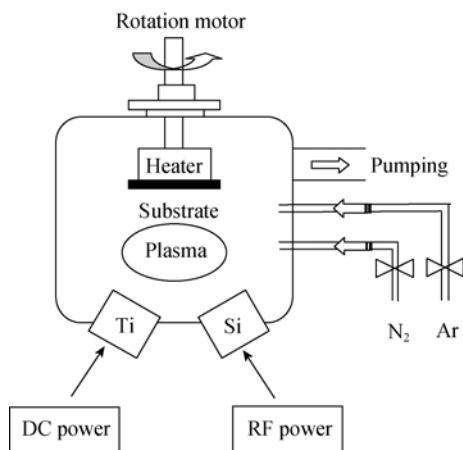


**Fig. 1** Schematic of the double-target magnetron co-sputtering system

Prior to the deposition, the system was firstly evacuated to a pressure of  $5.0 \times 10^{-4}$  Pa, and then the gases, whose flow rates were regulated by mass flow controllers, were introduced into the chamber with the total pressure maintained at  $5.0 \times 10^{-1}$  Pa. In order to further remove the surface contamination and oxidation, the substrates and the targets were sputter-cleaned in argon discharge with the negative bias voltage of 650 V for 10 min, respectively. The detailed deposition parameters were listed in Table 1. Two sets of

**Table 1** Deposition parameters of Ti-Si-N films by magnetron sputtering

Base pressure / Pa	$5.0 \times 10^{-4}$
Working pressure / Pa	$5.0 \times 10^{-1}$
Ar flow rate / ( $\text{ml} \cdot \text{min}^{-1}$ )	10
Ti: DC power / W	120
Si: RF power / W	80

samples were prepared: one set deposited at the  $N_2$  flow rate of  $20 \text{ ml} \cdot \text{min}^{-1}$  under the temperature of room temperature ( $11^\circ\text{C}$ ), 200, 300 and  $400^\circ\text{C}$ , and the other one deposited at  $300^\circ\text{C}$  under the  $N_2$  flow rate of 15, 20, 25 and  $30 \text{ ml} \cdot \text{min}^{-1}$ .

The crystalline quality and orientation of the samples were identified by X-ray diffraction (XRD) (D/Max-Ultima<sup>+</sup>). The composition and surface morphologies were performed by electron probe microanalyzer (EPMA) (Shimadzu, EPMA-1600) and atomic force microscope (AFM) (CSPM-5000), respectively. To examine the mechanical properties of these films, nanoindentation experiments were also carried out using Triboindenter (TI-950) system with a Berkovich diamond indenter. The thickness of the films was measured by Talysurf (CLI-2000).

## 3 Results and discussion

### 3.1 Structural properties

Figure 2 shows the XRD patterns of the Ti-Si-N films formed at different substrate temperature. It was found that all the Ti-Si-N films had a polycrystalline structure with crystal planes orientations of TiN (111) and TiN (200). However, the XRD patterns of our sputtered Ti-Si-N films show no peaks of  $\text{SiN}_x$  as shown in Fig. 2. This result

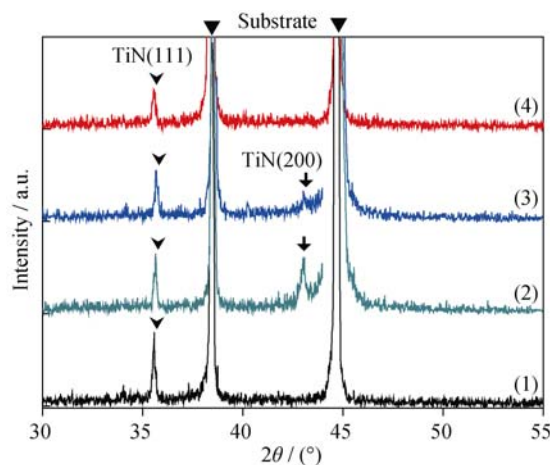


**Fig. 2** XRD patterns vs. temperature (1)  $11^\circ\text{C}$ ; (2)  $200^\circ\text{C}$ ; (3)  $300^\circ\text{C}$ ; (4)  $400^\circ\text{C}$

implied that N was present in a crystalline phase of TiN and an amorphous phase of SiN<sub>x</sub>. Hence, it is the characteristics of nano grains TiN embedded in an amorphous matrix SiN<sub>x</sub> which is called nanocomposite microstructure [6, 21–22]. The XRD peaks corresponding to TiN (200) plane were comparatively weak, compared to TiN (111) plane, originated from the diminution of grain size and the residual stress induced in the crystal lattice at the high content of Si. The primary TiN (200) diffraction peaks first become stronger and then weaker obviously with increasing substrate temperature from (1) room temperature 11 °C to (3) 300 °C. At last it disappeared in Fig. 2(4) with further increasing substrate temperature. Hence, the substrate temperature of 300 °C is an inflexion.

### 3.2 EPMA analysis

Figure 3 shows the elemental compositions of the Ti-Si-N films with respect to the N<sub>2</sub> flow rate. From the results, it can clearly be seen that the N contents in the films monotonically increased with the increasing of N<sub>2</sub> flow rate from 15 to 30 ml·min<sup>-1</sup>, while the Ti contents slightly decreased. It is speculated that amorphous SiN<sub>x</sub> is favored to form at the high N<sub>2</sub> flow rate. In order to investigate the effect of the N<sub>2</sub> flow rate on the existence of free Si in the films, Ti-Si-N films were deposited with different N<sub>2</sub> flow rate (from 20 to 30 ml·min<sup>-1</sup>) while almost same Si content of 28 wt.% due to the fixed ratio of Si target power compared to Ti target current. This result reflects that the nitriding of Si is fulfilled due to sufficient nitrogen supply.

### 3.3 Surface morphologies

In order to meet more practical application of Al alloy, Ti-Si-N films should have a very smooth surface, i.e. their surface roughness should reach less than 5 nm level. Here, Fig. 4 shows representative three-dimensional surface images of Ti-Si-N films at different temperature and N<sub>2</sub> flow rate. Four samples all displayed smooth surface profile dominated by domed features. The average root-mean-square (RMS) roughness is 0.38, 0.28, 0.67 and 0.46 nm

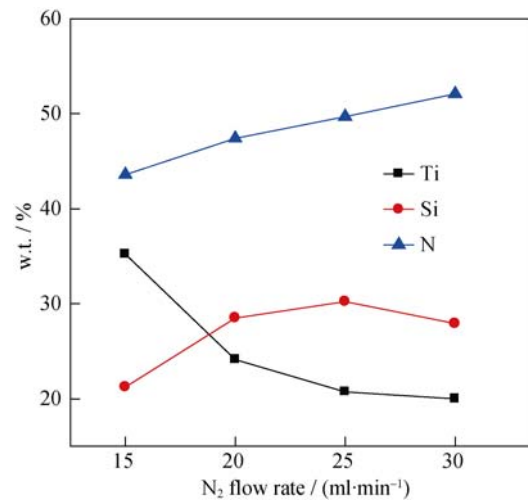


Fig. 3 Elemental contents vs. N<sub>2</sub> flow rate

while the grain size of the samples is 35, 28, 40 and 36 nm, respectively. The RMS surface roughness of Ti-Si-N thin film reaches an atomic level.

From Fig. 4, it is evident that, with increasing substrate temperature, grain size and surface roughness decrease, which could be explained from the XRD results. As the substrate temperature increases, the grain and column boundaries become denser, and then the smoother surface appears. We can also explain this temperature effect on the surface roughness by migration and diffusion of the reactants on the substrate surface. At lower substrate temperature, atoms assembled on the substrate surface have lower mobility, so the films showed a rougher surface; while increasing the substrate temperature, the migration ability of the atoms enhanced, leading to the increase of the surface smoothness. Besides that, with the N<sub>2</sub> flow rate changing from 15 to 30 ml·min<sup>-1</sup>, the surface smoothness of the films also becomes better. It leads to an observed smooth of the film for decreasing average grain size. From surface images analysis, AFM shows the RMS surface roughness of Ti-Si-N films is uniform under different substrate temperature and N<sub>2</sub> flow rate. What's more, the thin films deposited are all crystallized well, revealing smooth and lustrous appearance.

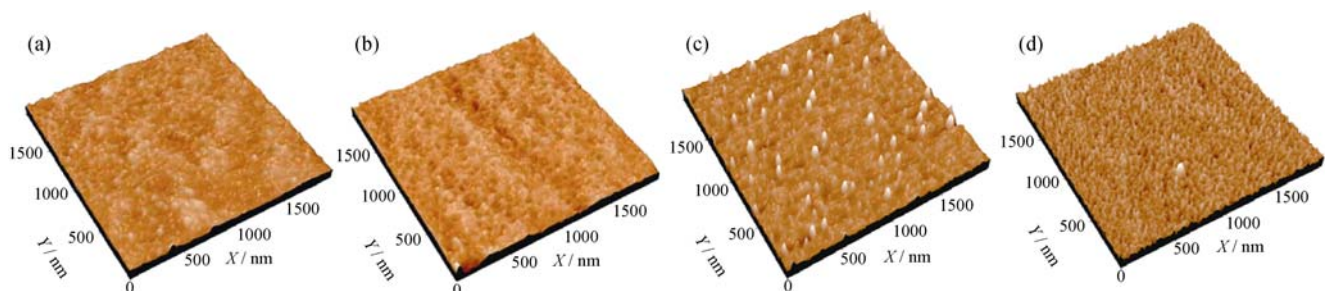


Fig. 4 AFM surface morphologies of Ti-Si-N thin films deposited at 300 °C and room temperature under the N<sub>2</sub> flow rate (a), (c) 15 ml·min<sup>-1</sup>; (b), (d) 30 ml·min<sup>-1</sup>

Furthermore, the thickness of the Ti-Si-N films as a function of  $N_2$  flow rate shows weak gas flow rate dependence (as shown in Fig. 5). The average thickness of the film is about 375 nm. This implies that the properties of Ti-Si-N films are thermally stable.

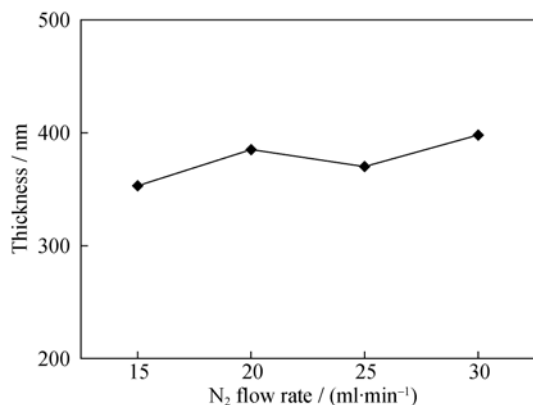


Fig. 5 Thickness of the Ti-Si-N films deposited at 300 °C

### 3.4 Nanohardness

It is reported that in the case of a hard film on a soft substrate, the plastic deformation easily extends into the substrate [3, 23–24]. The influence of the substrate on the hardness is small. With increasing the load force from 0.5 to 1.0 mN, the contact depth increases from 30 nm to about 50 nm, which was less than 13% of the obtained film thickness (350–400 nm) [25–26]. Figure 6 is the load-depth curve in the nanoindentation. In the test, the diamond Berkovich indenter was forced into the thin films under the load conditions. The loading profile during indentation testing was linearly increased by time and held 10 s at the peak load. On each sample nine separated indentations were taken, and the mean hardness and Young's modulus were calculated from the load-depth curve obtained from the nanoindentation testing. The measured nanohardness of the films shows an almost constant value. Thereby, the values are considered to be the hardness of the Ti-Si-N thin films.

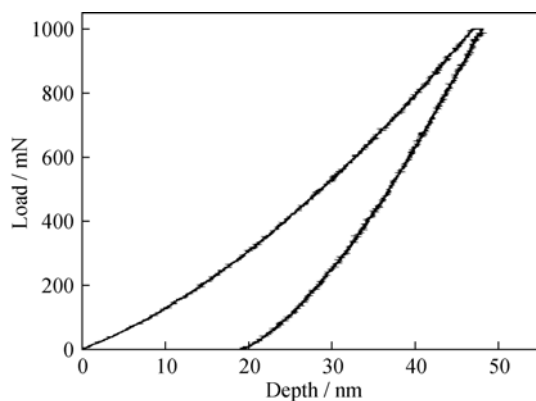


Fig. 6 Load-depth curve in the nanoindentation

Figure 7 shows the hardness and Young's modulus of the Ti-Si-N films measured by the nanoindentation techniques (TI-950, Hysitron) while obtained as a function of  $N_2$  flow rate. As the  $N_2$  flow rate increased, the hardness and Young's modulus steeply increased, with the maximum values about 27 and 254 GPa at the  $N_2$  flow rate of 25 ml·min<sup>-1</sup>, respectively, and then gradually reduced with further increasing the  $N_2$  flow rate. This behavior, in express of the linear hardness increase, could be explained by the more and more free Si nitrified into  $SiN_x$  with the increase of the  $N_2$  flow rate [13]. An enhancement of hardness, compared to the TiN films, was elucidated by the grain size effect of nanocrystals TiN embedded in the  $SiN_x$  amorphous matrix, which act as an effective barrier for dislocation motion. At the  $N_2$  flow rate of 30 ml·min<sup>-1</sup>, the hardness of the film is only 17 GPa, even lower than the values of 25 ml·min<sup>-1</sup>. With further increasing of the  $N_2$  flow rate from Fig. 7, the reduction of the hardness has been explained by the thickening of amorphous  $SiN_x$  phase due to complete nitrification of free Si. That is, the volume expansion compared to the case of free Si with same mole fraction may also cause the hardness reduction of a nanocomposite. This expansion subsequently increased the average free path of an amorphous phase in the composite, and thus decreased the hardness. This influence of  $N_2$  flow rate on the hardness of the Ti-Si-N films will be considered with crystallinity, microstructure, and chemical status of the Ti-Si-N films in the following research.

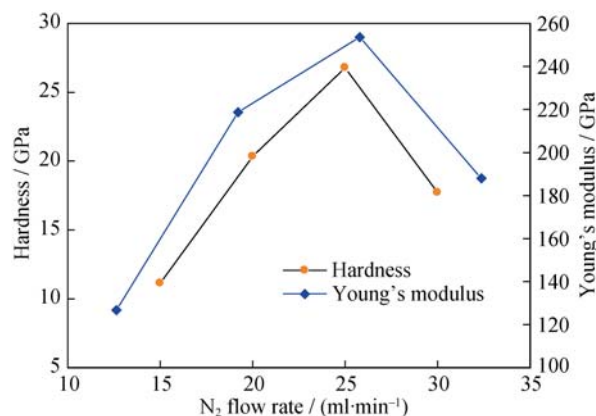


Fig. 7 Hardness and Young's modulus vs.  $N_2$  flow rate

### 3.5 Tribological properties

A test for friction coefficient was carried out with CEIR UMT-2 at a normal load of 300 mN and sliding speed of 1 mm·s<sup>-1</sup>. The Al substrate with Ti-Si-N films exhibited better tribological properties than the original substrate without any film. Figure 8 shows the friction coefficients of the films at 300 °C using  $Si_3N_4$  ball as a counterpart material. Friction coefficient varies between 0.70 and 0.85, as shown in Fig. 8. The effect of  $N_2$  flow rate on the adhesion of a film-substrate

system was evaluated by scratch adhesion testing. For the film tests presented in this research, excellent adhesion strength of Ti-Si-N films may play a positive role in the cutting performance. Generally, the films adhered well to the substrates. A proper amount of N in the Ti-Si-N films significantly improves the adhesion between the films and Al substrate.

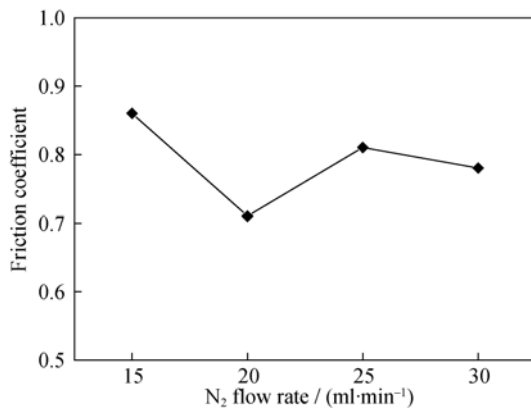


Fig. 8 Friction coefficient vs. N<sub>2</sub> flow rate at 300 °C

#### 4 Conclusion

Ti-Si-N thin films were prepared by a double-target magnetron co-sputtering system whose microstructure and mechanical property were affected by the N<sub>2</sub> flow rate and substrate temperature during co-sputtering. The thickness of the films shows weak gas flow rate dependent. With varying N<sub>2</sub> flow rate, the average thickness of the film is 375 nm approximately. The nanocomposite Ti-Si-N thin films, which have an amorphous microstructure with nano grains TiN embedded in an amorphous matrix SiN<sub>x</sub>, were revealed. The Ti-Si-N thin films show a smooth surface. With increasing the N<sub>2</sub> flow rate and substrate temperature, the surface of the films becomes smoother. The best RMS roughness obtained is 0.28 nm for the film. The maximum hardness and Young's modulus of the Ti-Si-N films are 27 and 254 GPa at the N<sub>2</sub> flow rate of 25 ml·min<sup>-1</sup>, respectively. With further increasing the N<sub>2</sub> flow rate, the hardness and Young's modulus were gradually reduced. As the substrate temperature and the N<sub>2</sub> flow rate sharply influence the microstructure of the films, they play important roles in the process of depositing Ti-Si-N thin films. From the results of this paper, magnetron sputtering is a promising method to deposit Ti-Si-N thin films onto the soft substrate.

#### Acknowledgement

This project was financially supported by the Cultivation Fund of the Key Scientific and Technical Innovation Project

and Ministry of Education of China (No. 707015).

#### References

- [1] Li L.H., Xia L.F., and Ma X.X., XPS of Ti+TiN+(N,C) multilayer films deposited by filtered cathodic arc deposition with controlled feed gas flow rate. *Surf. Coat. Tech.*, 1999, **120-121**: 618.
- [2] Gordani G.R., Shojarazavi R., Hashemi S.H., and Isfahani A.R.N., Laser surface alloying of an electroless Ni-P coating with Al-356 substrate. *Opt. Laser. Eng.*, 2008, **46** (7): 550.
- [3] Moy C.K.S., Cairney J., Ranzi G., Jahedi M., and Ringer S.P., Investigating the microstructure and composition of cold gas-dynamic spray (CGDS) Ti powder deposited on Al 6063 substrate. *Surf. Coat. Tech.*, 2010, **204** (23): 3739.
- [4] Rong P., Zhou H., Ning X., Lin Y., and Wei X., The study and fabrication of Al/AlN substrate. *Mater. Lett.*, 2002, **56** (4): 465.
- [5] Carvalho S., Ribeiro E., Rebouta L., Pacaud J., Goudeau P., Renault P.O., Rivière J.P., and Tavares C.J., PVD grown (Ti,Si,Al)N nanocomposite coatings and (Ti,Al)N/(Ti,Si)N multilayers: structural and mechanical properties. *Surf. Coat. Tech.*, 2003, **172** (2-3): 109.
- [6] Veprek S., Reiprich S., and Shizhi L. Superhard nanocrystalline composite materials: the TiN/Si<sub>3</sub>N<sub>4</sub> system. *Appl. Phys. Lett.*, 1995, **66** (20): 2640.
- [7] Cheng Y.H., Browne T., Heckerman B., and Xx X., Influence of Si content on the structure and internal stress of the nanocomposite TiSiN coatings deposited by large area filtered arc deposition. *J. Appl. Phys.*, 2009, **42** (12): 125415.
- [8] Zhang R.F., Sheng S.H., and Veprek S., Mechanical strengths of silicon nitrides studied by ab initio calculations. *Appl. Phys. Lett.*, 2007, **90** (19): 191903.
- [9] Chen Y., Lee K.W., Chiou W., Chung Y., and Keer L.M. Synthesis and structure of smooth, superhard TiN/SiN<sub>x</sub> multilayer coatings with an equiaxed microstructure. *Surf. Coat. Tech.*, 2001, **146-147**: 209.
- [10] Zou C.W., Wang H.J., Li M., Yu Y.F., Liu C.S., Guo L.P., and Fu D.J., Characterization and properties of TiN-containing amorphous Ti-Si-N nanocomposite coatings prepared by arc assisted middle frequency magnetron sputtering. *Vacuum.*, 2010, **84** (6): 817.
- [11] Jiang N., Shen Y.G., Mai Y.W., Chan T., and Tung S.C., Nanocomposite Ti-Si-N films deposited by reactive unbalanced magnetron sputtering at room temperature. *Mater. Sci. Eng. B.*, 2004, **106** (2): 163.
- [12] Zou C.W., Zhang J., Xie W., Shao L.X., and Fu D.J., Structure and mechanical properties of Ti-Al-N coatings deposited by combined cathodic arc middle frequency magnetron sputtering. *J. Alloy. Compd.*, 2011, **509** (5): 1989.
- [13] Shtansky D.V., Lobova T.A., Fominski V.Y., Kulinich S.A., Lyasotsky I.V., Petrzehik M.I., Levashov E.A., and Moore J.J. Structure and tribological properties of WSex, WSex/TiN, WSex/TiCN and WSex/TiSiN coatings. *Surf. Coat. Tech.*, 2004, **183** (2-3): 328.

- [14] Kim D., Svadkovski I., Lee S., Choi J., and Kim J., Synthesis Ti-Si-N nanocomposite coating prepared by a hybrid system of double bending filtered vacuum arc source and magnetron sputtering. *Curr. Appl. Phys.*, 2009, **9** (3-1): S179.
- [15] Mei F., Shao N., Hu X., Li G., and Gu M., Microstructure and mechanical properties of reactively sputtered Ti-Si-N nanocomposite films. *Mater. Lett.*, 2005, **59** (19-20): 2442.
- [16] Jiang N., Shen Y.G., Mai Y.W., Chan T., and Tung S.C., Nanocomposite Ti-Si-N films deposited by reactive unbalanced magnetron sputtering at room temperature. *Mat. Sci. Eng. B-Solid.*, 2004, **106** (2): 163.
- [17] Ahmed M.S., Zhou Z., Munroe P., Li L.K.Y., and Xie Z., Control of the damage resistance of nanocomposite TiSiN coatings on steels: roles of residual stress. *Thin Solid Films.*, 2011, **519** (15): 5007.
- [18] Bouzakis K.D., Skordaris G., Gerardis S., Katirtzoglou G., Makrimalakis S., Pappa M., Lili E., and M'Saoubi R., Ambient and elevated temperature properties of TiN, TiAlN and TiSiN PVD films and their impact on the cutting performance of coated carbide tools. *Surf. Coat. Tech.*, 2009, **204** (6-7): 1061.
- [19] Guo C.T., Lee D., and Chen P.C., Deposition of TiSiN coatings by arc ion plating process. *Appl. Surf. Sci.*, 2008, **254** (10): 3130.
- [20] Konofaos N., Angelis C.T., Evangelou E.K., Panayiotatos Y., Dimitriadis C.A., and Logothetidis S., Electrical characterization of TiN/aC/Si devices grown by magnetron sputtering at room temperature. *Appl. Phys. Lett.*, 2001, **78**: 1682.
- [21] Qiang R., and Shejun H., Effects of Ti<sub>(0.5)</sub>Al<sub>(0.5)</sub>N coatings on the protecting against oxidation for titanium alloys. *Rare Metals.*, 2010, **29** (2): 154.
- [22] Kim S.H., Kim J.K., and Kim K.H., Influence of deposition conditions on the microstructure and mechanical properties of Ti-Si-N films by DC reactive magnetron sputtering, [in] *Thin Solid Films Proceedings of the 29th International Conference on Metallurgic Coatings and Thin Films*, 2002, **420-421**: 360.
- [23] Wu Z., Bai Y., Qu W., Wu A., Zhang D., Zhao J., and Jiang X., Al-Mg-B thin films prepared by magnetron sputtering. *Vacuum.*, 2010, **85** (4): 541.
- [24] Cai X., and Bangert H., Hardness measurements of thin films-determining the critical ratio of depth to thickness using FEM. *Thin Solid Films.*, 1995, **264** (1): 59.
- [25] Tsui T.Y., Vlassak J., and Nix W.D., Indentation plastic displacement field: Part II. The case of hard films on soft substrates. *J. Mater. Res.*, 1999, **14** (06): 2204.
- [26] Wang J., Li W., Li H., Shi B., and Luo J., Nanoindentation study on the mechanical properties of TiC/Mo multilayers. *Thin Solid Films.*, 2000, **366** (1-2): 117.